Centrifugal Field-Induced Colloidal Assembly: From Chaos to Order

Mengdi Chen, Helmut Cölfen,* and Sebastian Polarz*

Department of Chemistry, University of Konstanz, Universitätsstrasse 10, 78457 Konstanz, Germany

ABSTRACT Given a certain binary phase, its crystal structure can usually be rationalized by thermodynamics and packing rules. However, there is still no fundamental understanding of how metastable solids form and how this is influenced by kinetic factors. Furthermore, the very early stages of crystallization remain vague. We present an experimental study using a binary mixture of colloidal particles as a model. Particle assembly is provoked by centrifugation, and the degree of separation can be adjusted precisely. Between the scenarios of random mixture (glassy state) and complete phase separation, conditions could be realized to facilitate the occurrence of various periodic structures in a single experiment. Some of these structures can only be explained by a dynamic, nonequilibrium and dissipative state. Eventually, the formation of certain metastable lattices can be interpreted as an emergent, systemic phenomenon. Thus, centrifugation can be used for studying the chaos–order transition in complex particle systems.

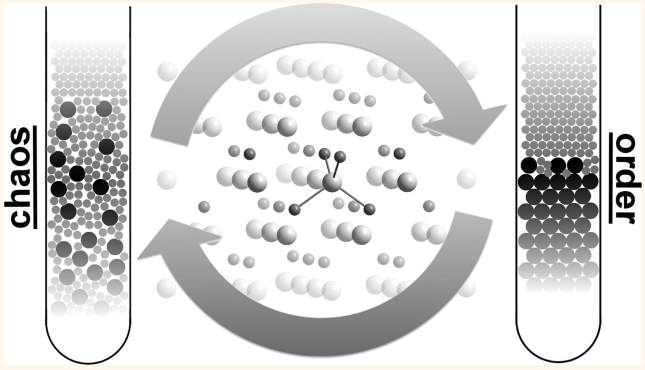

KEYWORDS: systems phenomena · colloidal model systems · nonclassical nucleation · analytical ultracentrifugation · self-assembly

The structure of any solid at the unit-cell dimension is a prevailing factor determining its properties, which is best represented by materials existing in different modifications (polymorphs, glasses), *e.g.*, carbon as an extreme case. It is highly important to understand, in depth, how and which modification forms and how to access potentially undiscovered forms.[1] For a system defined in composition, only one distinct modification can be explained solely by thermodynamic considerations; all other forms are the result of more or less marked, kinetic contributions. To this day, insights are rather empirical because the crystal structure is determined at the very early phases of the process, either at solidifaction from a dispersion or for amorphous–crystalline transitions. The lifespan of these early stages is short; they are far from equilibrium with highly dynamic character.[2,3] There is very limited information about the factors governing the very early stages of crystallization.[4,2] Whereas numerous methods exist for investigating the crystalline state, with diffraction methods leading the way, the precise characterization of an amorphous solid is extremely difficult.[5] Furthermore, a glass is also a rather vague term. What could make two glasses different and how to control the difference is still an open question.

In conclusion, it is highly desirable to obtain deep insights into the formation of glasses and metastable solids on the basis of experimental data. Because the latter is currently beyond reach for atomic systems, we follow a different approach here. It is well-known from literature that monodisperse colloidal particles can act as models for solid-state phenomena.[6–8] The advantage is the much easier accessibility of data as the colloidal particles used are typically several orders or magnitudes larger compared to atoms. Electron microscopy becomes a powerful tool for the investigation of the resulting solid materials. Most of the past attention was devoted to materials consisting of one size of spherical particles due to their special, photonic properties.[9,10] Different methods for colloidal assembly are known starting from colloidal dispersions like evaporation-induced self-assembly, electrophoresis, or centrifugation.[11–19] Using colloidal particles as supra-atoms enables the study of a range

* Address correspondence to helmut.coelfen@uni-konstanz.de, sebastian.polarz@uni-konstanz.de.

Received for review February 17, 2015 and accepted July 12, 2015.

Published online July 13, 2015
10.1021/acsnano.5b01116

of binary systems;[7,20,21] see also the excellent review articles by Möhwald *et al.* and by Stein *et al.*[22,23] In 2003, Kitaev and Ozin presented intriguing phases formed by polystyrene latex particles differing strongly in size (*e.g.*, 1.3 μm + 145 nm).[24] Park *et al.* have described a layer-by-layer technique for the generation of thin films of binary colloidal phases.[25] One should also note the work of Murray *et al.*, who have prepared highly ordered, binary lattices using inorganic nanocrystals and also those with nonspherical shape.[7,26] The resulting solids may then be interpreted as alloys, with glasses and solid solutions as the chaotic state and crystalline binary structures as ordered states.

In the current study, we use colloidal spheres (monodisperse, anionically stabilized polystyrene latex particles prepared using emulsion polymerization)[27] combined with centrifugation as a model system for studying the peculiarities of binary phases over a range of compositions. An advantage of this approach is that, unlike a classical crystallization experiment comprising atoms or ions, various parameters can be varied independent from each other, including kinetic parameters. The size d of the individual colloidal particles (d_{PS1}= 150 nm, d_{PS2} = 300 nm) and the quotient ($Q_{PF} = d_{PS1}/ d_{PS2}$) thereof was kept constant. First, we varied the total volume fraction of colloidal particles ($\Phi = \phi_{PS1} + \phi_{PS2}$) keeping their relative number ratio ($N = \phi_{PS1}/\phi_{PS2}$) constant because Φ comes closest to changing concentration in a classical crystallization experiment. Then, the centrifugal force F was changed as a kinetic parameter influencing how fast the particles sediment. The emerging structures were investigated using scanning electron microscopy (SEM) and were compared to classical solid-state crystals whenever possible. Finally, the outcome of an experiment with two successive steps with different centrifugal force was investigated.

RESULTS AND DISCUSSION

First, it is important to gain control over sedimentation and separation behavior of the binary system. Analytical ultracentrifugation (AUC) is a powerful tool to obtain *in situ* information about the sedimentation of the particles.[28] AUC was performed for dispersions varying in total volume fraction, and the monodisperse situation was compared to the binary case (Figure 1; see also S-2, Supporting Information). Several important conclusions can be extracted from the presented data. According to sedimentation theory, the concentration dependency of the sedimentation coefficient s for repulsive interaction between the particles is[29]

$$s = \frac{s^0}{(1 + k_s c)} \quad (1)$$

with $s^0 \cong$ the sedimentation coefficient at infinite dilution and $k_s \cong$ nonideality constant. The experimentally found sedimentation coefficients fit perfectly to the relationship given by eq 1. It seems that there are no special features apart from the expected nonideality even though two different sizes of the colloidal particles are present.[30]

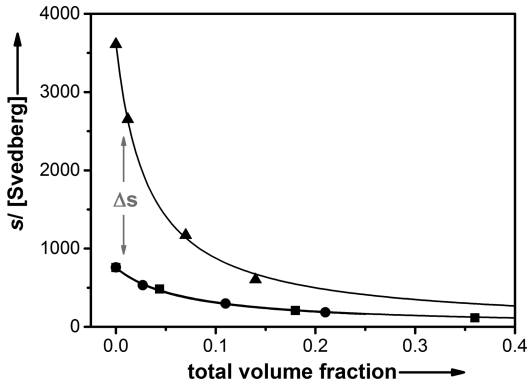

Figure 1. Φ dependency of the sedimentation coefficients. Circles $\cong$ monodisperse d_{PS1}, squares $\cong$ d_{PS1} in binary system $d_{PS1} + d_{PS2}$, triangles $\cong$ monodisperse d_{PS2}; solid lines $\cong$ theoretical data (eq 1).

With the data in Figure 1, it should be possible to differentiate between strong and weak separation conditions by the differences in the sedimentation coefficients of the two latices ($\Longrightarrow \Delta s$), depending on the combination of parameters $c_{PS1,2}$, Φ, and F and centrifugation time t_{CF} (see also S-3, Supporting Information). The results are shown in Figure 2. When separation is weak, only at the top of the centrifugation vial does one find a region consisting of separated smaller spheres PS1, which assemble into close packing (Figure 2a,b). The remaining, bottom part of the sample exists as a mixture of both sphere types in a disordered, glassy state. The presence of larger spheres in the matrix of the smaller spheres does obviously strongly prohibit the incurrence of crystalline domains, which fits to experimental and theoretical observations on binary colloidal systems made by others.[31,32] Closer inspection of the SEM images shows that there is a shallow gradient regarding the relative concentration of the two types of particles (see also S-4, Supporting Information).

The situation changes when conditions for strong separation conditions are selected (Figure 2e,f). PS1 and PS2 have formed separate domains, each predominantly close packed (face-centered cubic; see S-5, Supporting Information). Between these two extremes there is a situation shown in Figure 2c in which at the top and bottom of the centrifugation vial are densest packed zones. In between, a glassy, binary system can be found. The gradient in the particle size distribution function is more pronounced than before (S-4, Supporting Information). However, close to the medium separation scenario, one can find systems in which the entire binary phase is not completely disordered. Several binary zones possess periodic order (Figure 2d).

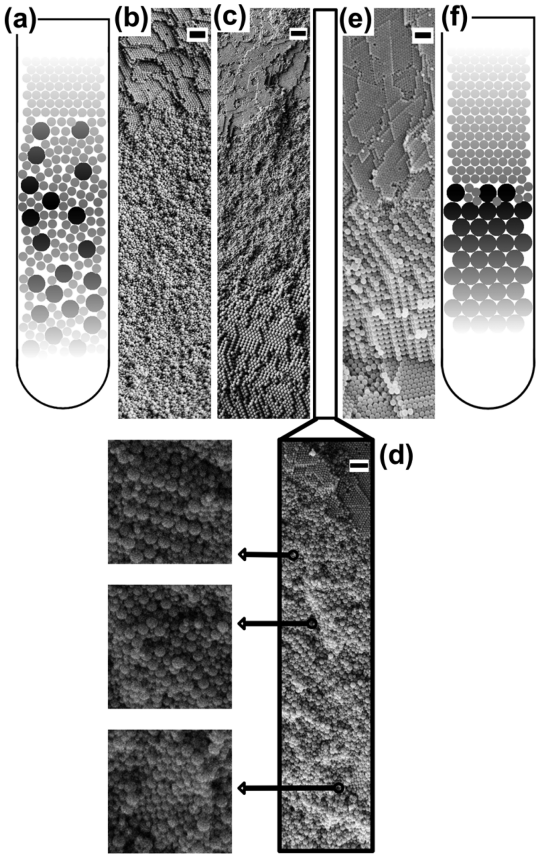

Figure 2. Schematic drawing and SEM micrographs showing different concentration gradients of the two sphere types (d_{PS1}, d_{PS2}) in the binary system caused by the adjustment of separation conditions (a, b ≅ weak; c, d ≅ medium; e,f ≅ strong). (d) Emergence of periodic binary features near the disorder → order transition. Scale bars ≅ 1 μm.

Because we wanted to explore the latter phenomenon in further depth, the remaining parameters like Q_{PF}, N, and most importantly the centrifugal force were varied. A subtle interplay between Δs and centrifugal force F is the central order parameter in the system. It is obvious that F directly influences the sedimentation rate. When sedimentation occurs very fast due to high centrifugal force (*e.g.*, $F = 1.2 \times 10^4$ g; g = earth's gravitational acceleration 9.81 m/s^2), the systems remain in the glassy state independent of Δs (see Figure 3a).

For small centrifugal force (*e.g.*, $F = 1.2 \times 10^2$ g), a significant fraction of the material exhibits the formation of a periodic (PS1)(PS2) structure shown in Figure 3b, consistent with the NaCl lattice (space group $Fm\bar{3}m$) (see S-6, Supporting Information). However, it must be noted that the assignment of crystal structures (3D information) from only one crystal plane [hkl] (2D information) is difficult and often not precise, and whenever possible one should take adjacent lattice planes into consideration. For instance, when seen exclusively from the [100] perspective, NaCl and CsCl look almost identical with a square unit pattern

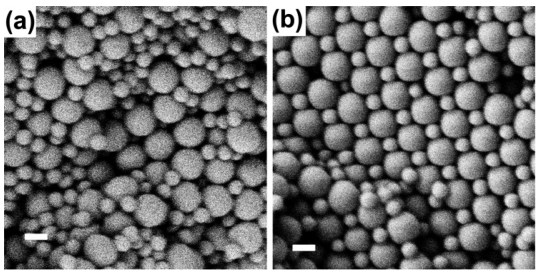

Figure 3. SEM micrographs of disordered binary structures obtained for large values of F (a) and ordered binary structures obtained for small values of F (b). Scale bars ≅ 200 nm.

(see Figure SI-7a, Supporting Information). However, from the side, it becomes clear that only in the case of NaCl the centers of small and large spheres are placed in plane, and for CsCl the small spheres are located below the top layer. From closer inspection of the SEM images (Figure 3 and Figure SI-7b, Supporting Information) it can be proven unequivocally that the rocksalt structure is present here. The emergence of the NaCl lattice is not surprising as it can be explained purely by packing arguments. $Q_{PF} = 0.5$ is very close to the ideal value (0.414) for the NaCl structure.[33] It is the thermodynamic optimum for this particular combination of particles. Therefore, the NaCl structure can even be obtained using only earth's gravitational field (S-8, Supporting Information).

However, for medium separation conditions and medium values of centrifugal force F (= 3.0×10^3 g), complexity explodes. A number of periodic, thermodynamically less stable structures (Figures 4 and 5) are observed. The emergence of such a variance of structures is in good agreement with a prediction made by Heras *et al.* in a theoretical paper in 2013, where the authors described phase diagrams of colloidal mixtures under gravity.[34] The structure shown in Figure 4a is in best agreement with a lattice based on a densely packed layer of the larger particles PS2. On top of this, the smaller spheres PS1 form a layer by regular filling of the voids of the PS2-layer. The structure is finalized by an additional PS2 layer on top. Comparison to structures related to atomic lattices shows that Figure 4a indicates a 1:2 stoichiometry akin to aluminum diboride (AlB_2; space group $P6/mmm$). Figure 4b can be rationalized by a small distortion involving a movement of the PS1 spheres closer to each other in a pairwise fashion (see S-9 Scheme 1, Supporting Information). The crystal domain shown in Figure 4b is slightly less symmetric, but it still has the $(PS1)_2(PS2)_1$ composition. The structure shown in Figure 4c cannot be related to AlB_2, which is hexagonal in nature with a hash-shaped a,b unit cell basis. The edges indicated in Figure 4c (see also S-9, Scheme 2, Supporting Information) allow identification of the *a*, *b*, *c* directions. The (001) plane is composed of four PS2 particles arranged in a quadratic fashion ($a = b = d_{PS2} = 300$ nm), centered by one PS1

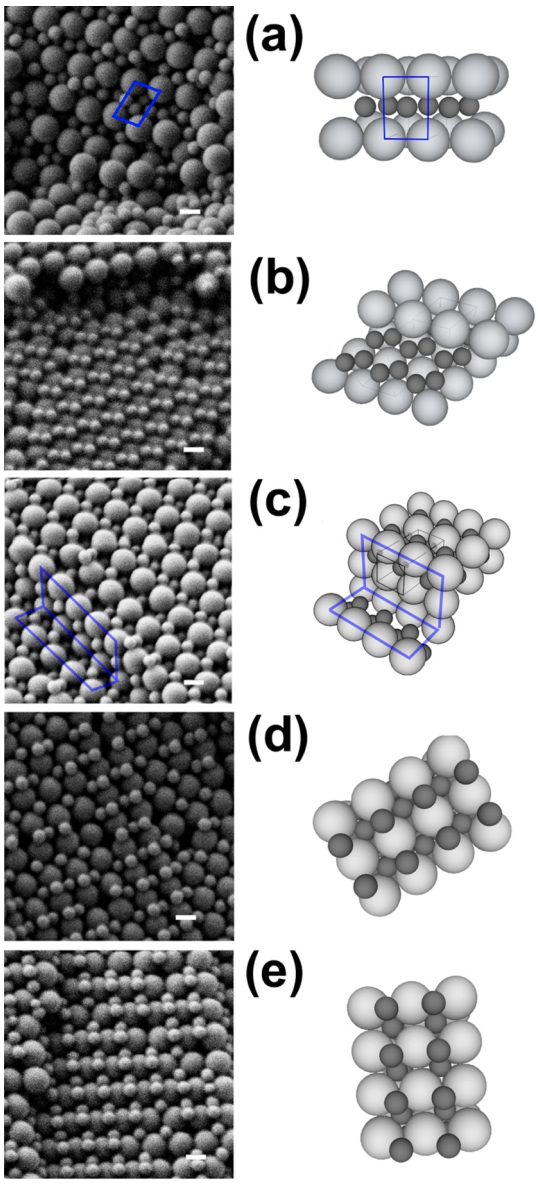

Figure 4. SEM micrographs and schematic of the crystal lattice for different ordered binary phases obtained *via* centrifugation: (a) layered structure akin to AlB_2; (b) distorted AlB_2 structure; (c) the tetragonal A_3B variant; the tetragonal A_2B variant before (d) and after distortion (e). Scale bars ≅ 200 nm.

sphere. Thus, the symmetry is no longer hexagonal as in AlB_2. The *c*-extension = 430 nm indicates that a tetragonal system is adopted. The isolated unit cell is shown in S-10 (Supporting Information) and corresponds to a $(PS1)_3(PS2)_1$ stoichiometry.

The ordered domains observed in Figure 4d can be explained starting from the latter structure by removing two symmetry equivalent spheres from the PS1-layer (S-9, Scheme 2 Supporting Information). This changes the stoichiometry to $(PS1)_2(PS2)_1$. Finally, because there is now more space in the [002] layer it can be observed that the PS1 particles are slightly changing their position (S-9, Scheme 3, Supporting Information), and the structure shown in Figure 4e is

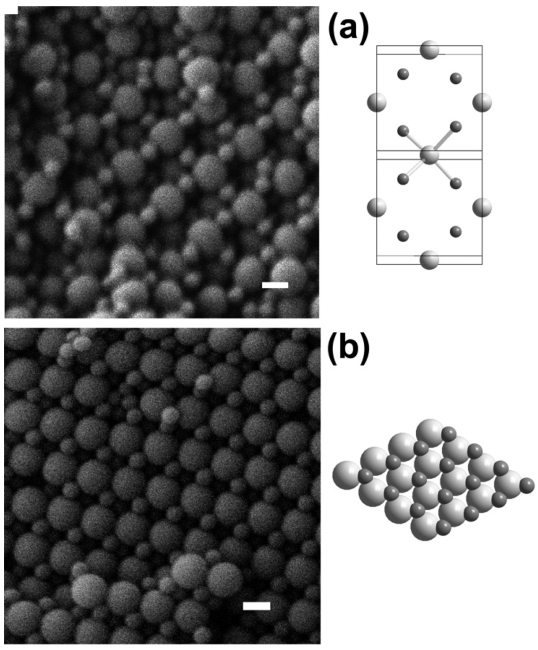

Figure 5. SEM micrographs of the nondense structures. Atomic analogue: sphalerite (a) and wurtzite structure (b). Scale bars ≅ 200 nm.

obtained. The possibility for the occurrence of thermodynamically less stable structures is best represented by a periodic structure characterized by the same stoichiometry compared to the NaCl structure (1:1) but with a much lower packing factor shown in Figure 5. Whereas the coordination mode in NaCl is (6/6), a tetrahedral (4/4) coordination can be clearly identified. The observed phase is in good agreement to the sphalerite structure ($F\bar{4}3m$). In addition to sphalerite a pattern can also be found that fits to the hexagonal analogue wurtzite ($P6_3mc$) (Figure 5b). Q_{PF} (= 0.5) is much too large compared to the ideal value for the sphalerite or wurtzite (0.225). Thus, the emergence of the shown structures with (4/4) coordination represents presumably the most astonishing and, thus, most significant result of our current study. It should be noted that the prevalence of the structures is very different. Whereas relatively large areas (>10 μm) associated with the more dense NaCl and AlB_2 structure can be found (see Figure S-11, Supporting Information), the other phases are present more seldom and are smaller. However, this result is rather expected. A precise quantification, which could help in assessing the relevance of thermodynamic *versus* kinetic factors, is not possible with our methods because the structures are present side by side, and SEM only gives information about the surface. It is not known at which position a domain is seen and how far the domain extends in 3-D.

Whereas all previous lattices (Figures 3b and 4) could be explained by packing considerations and stoichiometry influenced by the shallow concentration

gradient, despite centrifugation as a force for densification, sphalerite and wurtzite are clearly less dense structures. Furthermore, for hard colloidal particles with repulsive, spherical interaction potentials it is very hard to explain the low coordination number with local tetrahedral symmetry. The latter results are first indications that the mechanism leading to the various structures might be more complex than anticipated in the first place.

Further evidence for the latter hypothesis comes from the inspection of the entire length of the sedimentation body (Figure 2c,e and S-12, Supporting Information). At the bottom of the centrifugation tube a closest packed PS2 phase exists. This finding is unusual. Prior to centrifugation there is a homogeneous mixture of the two sphere types in the entire volume. When centrifugation and sedimentation begins, although the sedimentation coefficients s_{PS1} and s_{PS2} are different (Figure 1), small particles close to the bottom of the vial are expected to sediment together with the bigger ones to form a binary mixture (S-13, Supporting Information). However, the absence of PS1 in this region indicates that there must also be an upward movement, which removes the smaller particles from the bottom zone. This upward movement is not understandable in terms of the standard buoyancy term $(1 - \bar{\nu}\rho)$ used in the evaluation of (ultra)-centrifugation experiments with $\bar{\nu}$ = partial specific volume of the sample (0.949 mL/g for polystyrene) and ρ = solvent density since this predicts sedimentation of the polystyrene latexes because their density is higher than that of the solvent water. However, in our case, the solvent is not a one-component system anymore but a dispersion of host latexes and the situation becomes more complex.

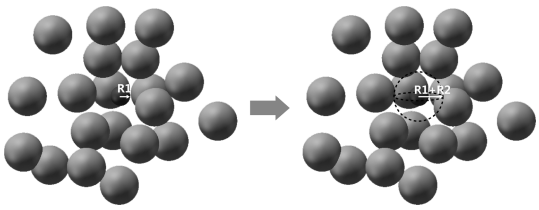

Figure 6. Schematic illustration of the effect of the insertion of a spherical guest particle of size R_1 into a colloidal dispersion of host particles with size R_2. The host particles are excluded from a volume that is larger than that of the guest particle volume V_1 by a factor of $(1 + R_2/R_1)^3$.

For concentrated binary dispersions, it has been pointed out that the buoyant force exerted on a sedimenting particle can be strongly affected by other components in the solution.[30] Our binary suspension can be regarded as a host (PS2) suspension containing guest particles (PS1). This situation is illustrated in Figure 6.

Since the guest particle is surrounded by a depletion layer of water with a density, which is lower than that of the surrounding host dispersion, it is understandable that a flotation of the guest particle can occur depending on the thickness of the depletion layer.[30] Indeed, it has been shown that very dense gold nanoparticles floated in a dispersion of polymer latexes. However, for a generic description, the simple excluded volume model can not be used and the buoyancy force can be calculated using density functional theory (DFT)[35] and the Mansoori–Carnahan–Starling equation of state for hard sphere mixtures yielding an equation for the effective density ρ^* of the host suspension[30]

$$\frac{\rho^* - \rho_0}{m_2' n_2} = \frac{6 - 2(2 - 3q)(1 - \Phi_2) - 3(1 - q^2)(1 - \Phi_2{}^2) + (1 - q)^2(2 + q)(1 - \Phi_2)^3}{2(4 - \Phi_2)\Phi_2 + (1 - \Phi_2)^4} \quad (2)$$

with

$$m_2' = (\rho_2 - \rho_0)v_{PS2} \quad (3)$$

$$n_2 = \frac{N_{PS2}}{V} \quad (4)$$

$$q = \frac{d_{PS2}}{d_{PS1}} \quad (5)$$

where $\rho_0 \cong$ density of the pure solvent, $\rho_2 \cong$ density of PS2 particle, m_2 = mass of PS2 particle $v_{PS2} \cong$ volume of a PS2 particle, n_2 = concentration of PS2 particles, $N_{PS2} \cong$ number of PS2, $V \cong$ total volume of the suspension, $\Phi_2 \cong$ volume fraction of the PS2 particles with $\Phi_2 = 1 - \Phi_1$, and d_{PS1} and d_{PS2} are the diameters of two kinds of particles, respectively.

When the volume fraction of the host particles exceeds a certain value, the effective density ρ^* of the solvent turns to be equal and higher than the density of the guest particles leading to their upward movement (flotation). This is the case at $\Phi_2 > 0.05$ for our investigated conditions, a concentration exceeded for the entire length of the column in the tube. The larger the particle size difference is, the more pronounced the flotation of the guest particles.[30] A yet unsolved key problem is to quantitatively experimentally observe the radial concentration gradients of both latexes in the mixture in the Analytical Ultracentrifuge. This would in principle be possible if the differently sized nanoparticles have different UV–vis markers. Detection of the concentration gradients would allow quantitative calculation of the radially dependent effective density ρ^* by eqs 2–5 and therefore the calculation of the entire concentration gradients. However, the strong light scattering of the PS2 prevents this even when using 60% sucrose to match the PS refractive index as closely as possible. The radial concentration gradients at high particle concentrations also hinder the calculation of a Peclet number for each

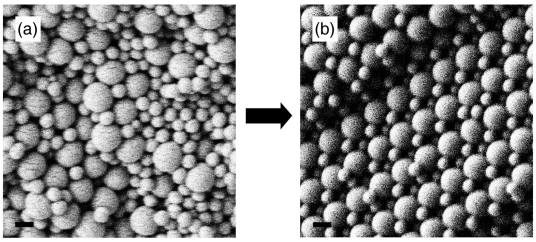

Figure 7. SEM micrographs for the two-step sedimentation experiment at $F = 1.2 \times 10^4$ g for 20 min first (a) followed by $F = 1.2 \times 10^2$ g for 5 h (b). Scale bars ≅ 200 nm.

particle size as is possible for diluted dispersions.[36] The reason is the concentration-dependent diffusion coefficient, which changes locally in the centrifuge tube and with it the Peclet number, which relates convection to diffusion.

The system seems to be more dynamic than we had expected. To test this, we performed a two-step sedimentation experiment. First, the dispersion was centrifuged at $F = 1.2 \times 10^4$ g for 20 min and then the same vial was centrifuged at $F = 1.2 \times 10^2$ g for 5 h. As described before, the first step leads to a binary, glassy state (Figure 7a). Next, although all colloidal particles have already sedimented, the second step leads to complete reorganization (Figure 7b). A periodic binary phase is observed.

Finally, we can compare the system presented here to other cases, for which the emergence of order from chaos has been reported. One famous example is the so-called Bénard experiment.[37] A thin film of a liquid is exposed to a temperature gradient, which is parallel to the direction of gravitation. Gravity tends to pull the denser liquid from top to bottom, while viscous damping force acts as a counter force. Depending on ΔT (the order parameter in the Bénard system), different and ordered patterns can emerge in the liquid. If ΔT is increased to be larger, the system would become more complex and chaotic. The situation in the presented centrifugation experiments of binary colloidal dispersions is similar. There is an overall sedimentation movement of the particles caused by the centrifugal field. The densification of the dispersion at the bottom of the centrifugation vial leads to an upward movement of the smaller particles PS1. The dynamic character, combined with the large number of interacting species and the steady supply with energy, due to the ongoing centrifugation, enables a dissipative state far from equilibrium, and this state is located near the disorder–order transition.

CONCLUSIONS

In this study, we were able to show that it is possible to create a structural gradient of a binary latex mixture including different glassy states but also different crystalline structures in a single centrifugation experiment. With the help of analytical ultracentrifugation as an in situ observation technique, we could precisely adjust the degree of separation of the colloidal particles with different size and, thus, also a concentration gradient. It was found that the centrifugal force is a crucial order parameter in the system. Besides the expected thermodynamically most stable structure and glassy states, a large number of different metastable polymorphs varying in stoichiometry were observed side by side in one experiment. Most importantly, considering that centrifugation is a process leading to densification, the occurrence of less-dense, low-coordinated structures like Sphalerite was very surprising. It could be shown that the emergence of periodic order is an emergent phenomenon resulting from nonequilibrium, dissipative conditions, which are commonly not considered in crystallization theories, but can be found for instance in systems like the Bénard cell known for the description of ordering phenomena in complex systems. Therefore, our current study poses the stimulating question, if besides packing factors and preference for coordination geometry also nonequilibrium, systemic features could influence the result of kinetically controlled crystallization process not only at the colloidal but also on the atomic scale. It seems that in the initial periods of a crystallization process in a binary system, even for a fixed size ratio of the particles, several polymorphs can form parallel to each other. Indeed, for $CaCO_3$, it was recently found that several nucleation pathways are simultaneously operative.[38]

METHODS

The monodisperse, negatively charged polystyrene microspheres were synthesized by emulsifier-free emulsion polymerization[27] and purified by dialysis. Binary colloidal structures of 150 nm (PS1) and 300 nm (PS2) latexes were fabricated with the L-70 ultracentrifuge (Beckman instruments) using the Beckman swing out rotor SW 55 Ti and ultra clear (5 × 41 mm) centrifuge tubes to maintain sedimentation as undisturbed as possible. After centrifugation, the remaining solvent at the top of the centrifuge tube was removed before the centrifuge tube was placed in a desiccator over silica gel for drying. The resulting structures were examined by cutting the dried samples with a razor blade along the long axis of the sample column, and the direction along the centrifugal force was subsequently investigated by using a Zeiss 249 CrossBeam 1540XB scanning electron microscope. A Beckman Optima XL-I analytical ultracentrifuge and a UV/vis multiwavelength analytical ultracentrifuge[39] developed as an open-source instrument[40] were used to measure the sedimentation coefficient of polystyrene spheres.

Conflict of Interest: The authors declare no competing financial interest.

Acknowledgment. M.C. is funded by a Chinese Scholarship Council stipend.

Supporting Information Available: ζ-Potential measurements for the different latex particles, concentration dependency of

sedimentation behavior studies by analytical ultracentrifugation, adjustment of different separation conditions, photographic images showing the development of separation with centrifugation time, schematic representation of the different concentration gradients obtained due to different separation conditions, transformation of different binary structures, investigation of the entire length of the sedimentation body, and schematic representation of the sedimentation process expected at the bottom of the centrifugation tube. The Supporting Information is available free of charge on the ACS Publications website at DOI: 10.1021/acsnano.5b01116.

REFERENCES AND NOTES

1. Jansen, M. A Concept for Synthesis Planning in Solid-State Chemistry. *Angew. Chem., Int. Ed.* **2002**, *41*, 3746–3766.
2. Pienack, N.; Bensch, W. In-Situ Monitoring of the Formation of Crystalline Solids. *Angew. Chem., Int. Ed.* **2011**, *50*, 2014–2034.
3. Demichelis, R.; Raiteri, P.; Gale, J. D.; Quigley, D.; Gebauer, D. Stable Prenucleation Mineral Clusters are Liquid-Like Ionic Polymers. *Nat. Commun.* **2011**, *2*, 590.
4. Gebauer, D.; Cölfen, H. Prenucleation Clusters and Non-Classical Nucleation. *Nano Today* **2011**, *6*, 564–584.
5. Greaves, G. N.; Sen, S. Inorganic Glasses, Glass-Forming Liquids and Amorphizing Solids. *Adv. Phys.* **2007**, *56*, 1–166.
6. Leunissen, M. E.; Christova, C. G.; Hynninen, A. P.; Royall, C. P.; Campbell, A. I.; Imhof, A.; Dijkstra, M.; van Roij, R.; van Blaaderen, A. Ionic Colloidal Crystals of Oppositely Charged Particles. *Nature* **2005**, *437*, 235–240.
7. Shevchenko, E. V.; Talapin, D. V.; Kotov, N. A.; O'Brien, S.; Murray, C. B. Structural Diversity in Binary Nanoparticle Superlattices. *Nature* **2006**, *439*, 55–59.
8. Yethiraj, A.; van Blaaderen, A. A Colloidal Model System with an Interaction Tunable from Hard Sphere to Soft and Dipolar. *Nature* **2003**, *421*, 513–517.
9. Joannopoulos, J. D.; Villeneuve, P. R.; Fan, S. H. Photonic Crystals: Putting a New Twist on Light. *Nature* **1997**, *386*, 143–149.
10. Wong, S.; Kitaev, V.; Ozin, G. A. Colloidal Crystal Films: Advances in Universality and Perfection. *J. Am. Chem. Soc.* **2003**, *125*, 15589–15598.
11. Murray, C. B.; Kagan, C. R.; Bawendi, M. G. Synthesis and Characterization of Monodisperse Nanocrystals and Close-Packed Nanocrystal Assemblies. *Annu. Rev. Mater. Sci.* **2000**, *30*, 545–610.
12. Holland, B. T.; Blanford, C. F.; Do, T.; Stein, A. Synthesis of Highly Ordered, Three-Dimensional, Macroporous Structures of Amorphous or Crystalline Inorganic Oxides, Phosphates, and Hybrid Composites. *Chem. Mater.* **1999**, *11*, 795–805.
13. Trau, M.; Saville, D. A.; Aksay, I. A. Assembly of Colloidal Crystals at Electrode Interfaces. *Langmuir* **1997**, *13*, 6375–6381.
14. Trau, M.; Saville, D. A.; Aksay, I. A. Field-Induced Layering of Colloidal Crystals. *Science* **1996**, *272*, 706–709.
15. Holgado, M.; Garcia-Santamaria, F.; Blanco, A.; Ibisate, M.; Cintas, A.; Miguez, H.; Serna, C. J.; Molpeceres, C.; Requena, J.; Mifsud, A.; Meseguer, F.; Lopez, C. Electrophoretic Deposition to Control Artificial Opal Growth. *Langmuir* **1999**, *15*, 4701–4704.
16. Denkov, N. D.; Velev, O. D.; Kralchevsky, P. A.; Ivanov, I. B.; Yoshimura, H.; Nagayama, K. 2-Dimensional Crystallization. *Nature* **1993**, *361*, 26–26.
17. Denkov, N. D.; Velev, O. D.; Kralchevski, P. A.; Ivanov, I. B.; Yoshimura, H.; Nagayama, K. Mechanism of Formation of 2-Dimensional Crystals from Latex- Particles on Substrates. *Langmuir* **1992**, *8*, 3183–3190.
18. Jiang, P.; Bertone, J. F.; Colvin, V. L. A Lost-Wax Approach to Monodisperse Colloids and Their Crystals. *Science* **2001**, *291*, 453–457.
19. Jiang, P.; Bertone, J. F.; Hwang, K. S.; Colvin, V. L. Single-Crystal Colloidal Multilayers of Controlled Thickness. *Chem. Mater.* **1999**, *11*, 2132–2140.
20. Redl, F. X.; Cho, K. S.; Murray, C. B.; O'Brien, S. Three-Fimensional Binary Superlattices of Magnetic Nanocrystals and Semiconductor Quantum Dots. *Nature* **2003**, *423*, 968–971.
21. Bartlett, P.; Ottewill, R. H.; Pusey, P. N. Superlattice Formation in Binary-Mixtures of Hard-Sphere Colloids. *Phys. Rev. Lett.* **1992**, *68*, 3801–3804.
22. Wang, D. Y.; Möhwald, H. Template-Directed Colloidal Self-Assembly - The Route to 'Top-Down' Nanochemical Engineering. *J. Mater. Chem.* **2004**, *14*, 459–468.
23. Li, F.; Josephson, D. P.; Stein, A. Colloidal Assembly: The Road from Particles to Colloidal Molecules and Crystals. *Angew. Chem., Int. Ed.* **2011**, *50*, 360–388.
24. Kitaev, V.; Ozin, G. A. Self-Assembled Surface Patterns of Binary Colloidal Crystals. *Adv. Mater.* **2003**, *15*, 75–78.
25. Kim, M. H.; Im, S. H.; Park, O. O. Fabrication and Structural Analysis of Binary Colloidal Crystals with Two-Dimensional Superlattices. *Adv. Mater.* **2005**, *17*, 2501–2505.
26. Dong, A. G.; Chen, J.; Vora, P. M.; Kikkawa, J. M.; Murray, C. B. Binary Nanocrystal Superlattice Membranes Self-Assembled at the Liquid-Air Interface. *Nature* **2010**, *466*, 474–477.
27. Reese, C. E.; Guerrero, C. D.; Weissman, J. M.; Lee, K.; Asher, S. A. Synthesis of Highly Charged, Monodisperse Polystyrene Colloidal Particles for the Fabrication of Photonic Crystals. *J. Colloid Interface Sci.* **2000**, *232*, 76–80.
28. Planken, K. L.; Cölfen, H. Analytical Ultracentrifugation of Colloids. *Nanoscale* **2010**, *2*, 1849–1869.
29. Harding, S. E., Rowe, A. J., Horton, J. C., Eds. *Analytical Ultracentrifugation in Biochemistry and Polymer Science*; Royal Society of Chemistry: London, 1992; p 629.
30. Piazza, R.; Buzzaccaro, S.; Secchi, E.; Parola, A. On the General Concept of Buoyancy in Sedimentation and Ultracentrifugation. *Phys. Biol.* **2013**, *10*, 045005.
31. Sentjabrskaja, T.; Babaliari, E.; Hendricks, J.; Laurati, M.; Petekidis, G.; Egelhaaf, S. U. Yielding of Binary Colloidal Glasses. *Soft Matter* **2013**, *9*, 4524–4533.
32. Voigtmann, T. Multiple Glasses in Asymmetric Binary Hard Spheres. *Epl* **2011**, *96*, 36006.
33. Chen, M.; Cölfen, H.; Polarz, S. The Effect of Centrifugal Force on the Assembly and Crystallization of Binary Colloidal Systems: Towards Structural Gradients. *Z. Naturforsch., B: J. Chem. Sci.* **2013**, *68*, 103–110.
34. de las Heras, D.; Schmidt, M. The Phase Stacking Diagram of Colloidal Mixtures under Gravity. *Soft Matter* **2013**, *9*, 8636–8641.
35. Hansen, J. P.; I.R, M. *Theory of Simple Liquids*, 3rd ed.; Elsevier: Amsterdam, 2006.
36. Benes, K.; Tong, P.; Ackerson, B. J. Sedimentation, Peclet number, and Hydrodynamic Screening. *Phys. Rev. E* **2007**, 10.1103/PhysRevE.76.056302.
37. Cross, M. C.; Hohenberg, P. C. Pattern-Formation outside of Equilibrium. *Rev. Mod. Phys.* **1993**, *65*, 851–1112.
38. Nielsen, M. H.; Aloni, S.; De Yoreo, J. J. *In situ* TEM Imaging of CaCO3 Nucleation Reveals Coexistence of Direct and Indirect Pathways. *Science* **2014**, *345*, 1158–1162.
39. Strauss, H. M.; Karabudak, E.; Bhattacharyya, S.; Kretzschmar, A.; Wohlleben, W.; Colfen, H. Performance of a Fast Fiber Based UV/Vis Multiwavelength Detector for the Analytical Ultracentrifuge. *Colloid Polym. Sci.* **2008**, *286*, 121–128.
40. Cölfen, H.; Laue, T. M.; Wohlleben, W.; Schilling, K.; Karabudak, E.; Langhorst, B. W.; Brookes, E.; Dubbs, B.; Zollars, D.; Rocco, M. The Open AUC Project. *Eur. Biophys. J.* **2010**, *39*, 347–359.